International Journal of Innovative Computing, Information and Control
Volume **19**, Number **1**, February **2023**

ICIC International ©2023 ISSN 1349-4198
pp. **139–151**

IMMERSION AND INVARIANCE CONTROL DESIGN FOR HYBRID EXCITATION SYNCHRONOUS MACHINES

Ekkachai Mujjalinvimut[1] and Adirak Kanchanaharuthai[2,*]

[1]Department of Electrical Engineering
Faculty of Engineering
King Mongkut's University of Technology Thonburi
Pracha Uthit Road, Bang Mod, Bangkok 10140, Thailand
ekkachai.muj@kmutt.ac.th

[2]Department of Electrical Engineering
College of Engineering
Rangsit University
52/347 Muang-Ake, Phaholyothin Rd., Lak-Hok, Muang, Patumthani 12000, Thailand
*Corresponding author: adirak@rsu.ac.th

Received June 2022; revised September 2022

Abstract. *A nonlinear feedback stabilizing controller technique for a hybrid excitation synchronous machine (HESM) system is developed in this study. The desired control law is designed using the immersion and invariance (I&I) technique. To ensure that the equilibrium point is asymptotically stable and that all the overall closed-loop system trajectories are bounded, the developed control mechanism is applied. A nonlinear dynamical system of the HESM is used to demonstrate the technique's effectiveness and practicality. The simulation findings show that the approach can track speed even when there is a sudden load torque. It has the ability to reduce oscillations quickly and surpass the existing nonlinear backstepping controller.*

Keywords: Nonlinear control, Immersion and invariance, Hybrid excitation synchronous machine, Backstepping

1. **Introduction.** The HESM was first proposed in [1]. The structure of HESM differs from that of general excitation synchronous machines and permanent magnet synchronous machines. It possesses a permanent magnet and field winding, and its two sources of magnetization are concurrent. It has a broad development potential since it combines the benefits of both permanent-magnet machines and excitation machines. Unfortunately, the HESM is a strongly coupled extremely nonlinear multi-variable system. The high nonlinearity is caused by the coupling between speed and armature currents, and perturbations such as inadequate modeling of uncertain parameters (armature winding resistance, moment of inertia and so on), as well as errors caused by sensors (angular position, angular velocity), and discretization influences (delay, numerical errors).

As considerable effort has been done on saving energy and broad timing drive systems, HESM has recently gained increased attention and has become one of the new research hotspots. The majority of current HESM research [2, 3, 4] has been on machine design, manufacturing, and test analysis, with little mention of speed regulation. Because the HESM system is affine in control, it is natural to apply nonlinear system geometric theory to it. The HESM system is locally weakly controllable, strongly accessible, and locally weakly observable, which are the key findings. Also, it is both input-output invertible and

DOI: 10.24507/ijicic.19.01.139

linearizable. As a result, a linear control strategy works well with the HESM. The linear control technique is obtained by accurately eliminating nonlinear terms, which will result in performance degradation. Moreover, the linear control approach cannot guarantee the stability of a system when the equivalent equilibrium point, such as unknown parameters or changing environmental temperatures, is changed. As a result, the linear control technique will fail to ensure global stability within the servo drive's scope.

To the best of the author's knowledge, relatively little work has been devoted directly applying nonlinear control theory to the construction of a feedback stabilizing nonlinear controller for the HESM. An adaptive backstepping controller [5] for the HESM was developed to deal with nonlinear coupling and parameter uncertainties and to make the HESM rotor speed track the desired rotor speed. Even if the resulting control law was effective, it relied upon selecting the virtual control functions and its derivatives in each step design to find out the final controller. In [6], a nonlinear $\mathcal{H}_\infty$ controller design for hybrid excited synchronous generators through AC/DC and DC/AC converters has been presented with the help of the approximate linearization around a temporary operting point. Sun et al. [7] proposed a feedback linearization decoupling sliding mode controller design for a hybrid excitation synchronous generator motor. The obtained controller provided enhanced dynamic responses and decreased the torque and current ripples despite the load disturbances. However, it was designed via feedback linearization method.

According to the aforementioned research, even if the nonlinear controller design strategies above are effective, there are important disadvantages. In particular, backstepping design is based on finding its derivatives in each step design to determine the final controller, leading to the complexity problem in the design procedure. According to the result of [6], the developed control was designed via the linearizing method, which may degrade the system performance while changing the operating point. In [7], the presented control relied on the combination of the feedback linearization method and sliding mode design, which needs to select the output function and the sliding surface function to find the desired controller. However, a suitable selection of both functions is not systematic.

This research therefore follows this line of investigation and focuses on an advanced nonlinear controller design to make the rotor speed track the reference rotor speed for the nonlinear HESM model. An immersion and invariance (I&I) control approach [8, 9] is used to design the controller in this paper. The I&I control method's control goal is to find a stabilizing feedback controller. The obtained controller in this research can deal with the "explosion of complexity" problem arising in backstepping and has the systematic design procedure. Furthermore, the presented control outperforms backtepping control because it can achieve high-performance speed tracking with asymptotic tracking with zero error.

As the above discussion, the followings are the main contributions of this work.

- An immersion and invariance control technique is proposed to tackle the HESM speed tracking control problem, which has yet to be investigated, using a nonlinear HESM dynamic model.
- With the help of Lyapunov theory, the closed-loop system's signals are all bounded, and the asymptotic tracking is achieved.
- The developed design technique is not complicated but effective and systematic when compared to backstepping controller. In addition, the suggested controller shows superior dynamic performance, such as less overshoot and faster oscillation reduction.

The rest of this paper is organized as follows. Section 2 presents a brief presentation of dynamic model of the HESM system and the problem statement. Nonlinear I&I control design is provided in Section 3. In Section 4, the simulation results are given to show the effectiveness of the developed design. Finally, the paper is concluded in Section 5.

2. **HESM System Model.** In the synchronously rotating rotor d-q coordinates, the hybrid excitation synchronous machine [5, 7] can be characterized by the following dynamical equations:

$$\begin{cases} \dot{\omega} &= \dfrac{R_\Omega}{J}\omega + \dfrac{P_n}{J}(L_d - L_q)i_q i_d + \dfrac{P_n\Phi_a}{J}i_q + \dfrac{P_n M_f}{J}i_q i_f - \dfrac{1}{J}T_l, \\ \dot{i}_d &= -L_f RKi_d + L_f L_q K P_n \omega i_q + M_f R_f K i_f + L_f K u_d - M_f K u_f, \\ \dot{i}_q &= \dfrac{-L_d}{L_q}P_n\omega i_d - \dfrac{R}{L_q}i_q - \dfrac{M_f}{L_q}P_n\omega i_f - \dfrac{\Phi_a}{L_q}P_n\omega + \dfrac{1}{L_q}u_q, \\ \dot{i}_f &= -M_f RKi_d - M_f L_q K P_n \omega i_q - L_f R_f K i_f - ML_f K u_d - L_d K u_f \end{cases} \tag{1}$$

with $K = \frac{1}{L_d L_f - M_f^2}$, where u_d, u_q, and u_f denote the d- and q-axes stator, and auxiliary excitation winding voltages, respectively. i_d, i_q, and i_f denote d- and q-axes stator, and auxiliary excitation winding currents, respectively. R and R_f represent stator per-phase and auxiliary excitation winding resistances, respectively; L_d, L_q, and L_f are d- and q-axes stator, and auxiliary excitation winding inductances, respectively; M_f denotes the mutual induction between auxiliary excitation winding and d-axis winding; Φ_a represents the flux linkage of rotor permanent-magnet; P_n denotes the number of poles of the machine; ω denotes the rotor speed in angular frequency; J represents the moment of inertia of the machine and load; R_Ω is the friction coefficient of the machine; and T_l represents the load torque.

Remark 2.1. *In this study, even though the load torque T_l, the friction coefficient R_Ω, and the moment of inertia J are regarded as constant values, these parameters are unknown in practical HESM systems. The authors assumed that they are constants for only simplicity to design the I&I-based controller. For future work, an adaptive I&I control design to estimate these unknown parameters will be developed.*

It can be observed that the input variables u_d, u_q, and u_f are used in the HESM model. These variables are suitable for the HESM system that is controlled by the voltage source. The inputs to the model are affine, and no inputs appear in the first subsystem of (1).

In order to simplify the state-space equation of the system (1), let us introduce the following state variables:

$$x_1 = \omega - \omega_r, \quad x_2 = i_d, \quad x_3 = i_q, \quad x_4 = i_f \tag{2}$$

where ω_r denotes the reference input which needs to be tracked.

Therefore, we have the state variable vector employed in this design procedure as $x = [x_1, x_2, x_3, x_4]^T$. After differentiating the state variables above, the dynamic model of the nonlinear HESM system can be rewritten as an affine nonlinear system as follows.

$$\dot{x} = f(x) + g(x)u(x) \tag{3}$$

with

$$f(x) = \begin{bmatrix} f_1(x) \\ f_2(x) \\ f_3(x) \\ f_4(x) \end{bmatrix} = \begin{bmatrix} \dfrac{R_\Omega}{J}(x_1 + \omega_r) + \dfrac{P_n}{J}(L_d - L_q)x_2 x_3 + \dfrac{P_n\Phi_a}{J}x_3 + \dfrac{P_n M_f}{J}x_3 x_4 - \dfrac{T_l}{J} \\ -L_f RKx_2 + L_f L_q K P_n \omega x_3 \\ \dfrac{-L_d}{L_q}P_n\omega x_2 - \dfrac{R}{L_q}x_3 - \dfrac{M_f}{L_q}P_n\omega x_4 - \dfrac{\Phi_a}{L_q}P_n\omega \\ M_f RKx_2 - M_f L_q K P_n \omega x_3 - L_f R_f K x_4 \end{bmatrix}$$

$$g(x) = \begin{bmatrix} 0 & 0 & 0 \\ g_{21}(x) & 0 & g_{23}(x) \\ 0 & g_{32}(x) & 0 \\ g_{41}(x) & 0 & g_{43}(x) \end{bmatrix} = \begin{bmatrix} 0 & 0 & 0 \\ L_f K & 0 & -M_f K \\ 0 & \dfrac{1}{L_q} & 0 \\ -M_f K & 0 & L_d K \end{bmatrix}, \quad u(x) = \begin{bmatrix} u_d \\ u_q \\ u_f \end{bmatrix} \tag{4}$$

In addition, the region of operation is defined in the set $\mathcal{D} = \{x \in \mathbb{R} \times \mathbb{R} \times \mathbb{R} \times \mathbb{R}\}$. The open loop operating equilibrium is denoted by $x_e = [x_{1e},\ x_{2e},\ x_{3e},\ x_{4e}]^T = [0,\ i_{de},\ i_{qe},\ i_{fe}]^T$.

Problem statement: The aim of this paper is to develop a nonlinear control voltage $u(x)$ for the HESM model with the help of immersion and invariance method. The developed controller satisfies the followings: (i) the HESM rotor speed ω is capable of tracking the desired rotor speed ω_r and (ii) the overall closed-loop system is asymptotically stable at the desired equilibrium (x_e). And all the resulting closed-loop responses are bounded.

The following assumption and lemma are established in order to satisfy these required objectives above.

Assumption 2.1. *All state variables $x_1, x_2, x_3, x_4 \in \mathbb{R}$ are assumed to be measurable.*

Lemma 2.1. [10] *If the constants $p > 1$ and $q > 1$ are such that $(p-1)(q-1) = 1$, then for all $\epsilon > 0$ and all $(x, y) \in \mathbb{R}^2$ we have*

$$xy \leq \frac{\epsilon^p}{p}|x|^p + \frac{1}{q\epsilon^q}|y|^q \tag{5}$$

If choosing $p = q = 2$ and $\epsilon^2 = 2\kappa$, the inequality above becomes

$$xy \leq \kappa x^2 + \frac{1}{4\kappa}y^2 \tag{6}$$

For the developed design procedure in the next section, the I&I control design will be developed to obtain a feedback stabilizing nonlinear control. In the following section, the developed control is designed step by step to achieve the desired performances.

3. Nonlinear Control Design.

This section introduces the concepts of immersion and invariance (I&I). This section establishes the nonlinear I&I control algorithm for the HESM model. The significant advancements are described in depth in the following two subsections. The I&I control technique is described in the first subsection. The second one is broken down into five parts: (i) select a target system with a lower dimension than the one under consideration, (ii) find three mapping functions $\pi_2(x_1)$, $\pi_3(x_1)$, and $\pi_4(x_1)$, (iii) establish an implicit manifold, (iv) check manifold attractivity and trajectory boundedness, and (v) determine the required control law.

3.1. Immersion and invariance control scheme.

Immersion and invariance in controller design is an advanced control method. The I&I technique, which was first introduced in [8, 9], is advantageous for nonlinear system design, stabilization, and adaptive control. The most important part of the I&I design is to immerse the original dynamical system into a target system that can capture the behavior that is wanted from the system. The method is based on the concepts of invariant manifolds and system immersion, according to a generalized description. The original state variable of the system, $x(t)$, is changed into two new state variables, $\xi(t)$ and $z(t)$. A state whose dimension $\xi(t)$ is strictly lower than the state $x(t)$ is the pre-specified target system. The transformation that is used to introduce the two states indicated above also describes the system's invariant manifold. The off-the-manifold state is a complement to the dimension of $\xi(t)$ and is referred to as $z(t)$. The purpose of this technique is to find a stabilizing nonlinear

feedback controller that keeps the original state $x(t)$ bounded, the manifold invariant, and the off-line manifold state $z(t)$ asymptotically approaches the desired equilibrium. Furthermore, the original state $x(t)$ will settle to the desired equilibrium points with a dynamic behavior similar to the goal dynamics.

This method can be used to address real-world challenges in controller design for a wide range of systems, such as power systems [11, 12, 13, 14, 15], induction motors [16], quadrotors [17], DC-DC converters [18], unmanned aerial vehicles (UAVs) [19], flywheel energy storage systems [20], and congestion tracking control for wireless TCP/AQM networks [21].

The interested reader is recommended to [9] for additional information as well as examples of applications that are used in the real world.

The immersion and invariance strategy of a nonlinear controller design has never been explored before for the nonlinear HESM model. In this study, the I&I technique is used to suggest a nonlinear controller for the HESM. The following results [8, 9] will be utilized to design a nonlinear controller for the HESM model.

Theorem 3.1. [8, 9] *Consider the nonlinear system*[1]

$$\dot{x}(t) = f(x) + g(x)u(x) \tag{7}$$

with state $x \in \mathbb{R}^n$ and control input $u \in \mathbb{R}^m$, and an assignable equilibrium point $x_e \in \mathbb{R}^n$ to be stabilized. Let $s < n$, and assume that there exist smooth mappings $\alpha : \mathbb{R}^s \to \mathbb{R}^s$, $\pi : \mathbb{R}^s \to \mathbb{R}^n$, $c : \mathbb{R}^n \to \mathbb{R}^m$, $\phi : \mathbb{R}^n \to \mathbb{R}^{n-s}$, $\varphi : \mathbb{R}^{n\times(n-s)} \to \mathbb{R}^m$, such that the followings hold.

(H1) (Target system) The system

$$\dot{\xi} = \alpha(\xi) \tag{8}$$

with state $\xi \in \mathbb{R}^s$, has an asymptotically stable equilibrium at $\xi_e \in \mathbb{R}^s$ and $x_e = \pi(\xi_e)$.

(H2) (Immersion condition) For all $\xi \in \mathbb{R}^s$

$$f(\pi(\xi)) + g(\pi(\xi))c(\pi(\xi)) = \frac{\partial \pi(\xi)}{\partial \xi}\alpha(\xi) \tag{9}$$

(H3) (Implicit manifold) The set identity

$$\begin{aligned} \mathcal{M} &:= \{x \in \mathbb{R}^n |\ x = \pi(\xi) \text{ for some } \xi \in \mathbb{R}^s\} \\ &= \{x \in \mathbb{R}^n |\ \phi(x) = 0\} \end{aligned} \tag{10}$$

holds.

(H4) (Manifold attractivity and trajectory boundedness) All trajectories of the system

$$\begin{aligned} \dot{z} &= \frac{\partial \phi(x)}{\partial x}[f(x) + g(x)\varphi(x,z)] \\ \dot{x} &= f(x) + g(x)\varphi(x,z) \end{aligned} \tag{11}$$

are bounded and satisfy

$$\lim_{t\to\infty} z(t) = 0 \tag{12}$$

where $z = \phi(x)$ and $u = \varphi(x, z)$.

Then, x_e is an asymptotically stable equilibrium of the closed-loop dynamics

$$\dot{x} = f(x) + g(x)\varphi(x, \phi(x)).$$

Refer to the proof of Theorem 3.1 [9] for more details. The following is a summary and interpretation of Theorem 3.1. The objective, given the original system and the

[1]It is assumed that all functions and mapping are smooth, i.e., $\mathbb{C}^\infty$, throughout this paper.

target dynamical system, is to determine a manifold $\mathcal{M}$ satisfying the condition (H3). This manifold can be rendered invariant and asymptotically stable. Also, it is such that the well-defined restriction of the closed-loop dynamics to $\mathcal{M}$ which is described by the selected target dynamics. Additionally, the control input u, which is capable of invariantly defining the manifold, is not unique, as it is defined uniquely on only $\mathcal{M}$. According to condition (H4), one of the possible controllers can be chosen to drive the off-manifold coordinate z to zero while simultaneously keeping the system signals bounded.

3.2. **I&I controller design.**

3.2.1. *Target system.* In accordance with Theorem 3.1's requirement (H1), we design the target system $\dot{\xi} = \alpha(\xi)$ as a one-dimension system that must be immersed in the four-dimension one.

As the selected target dynamics as given in (13) in this paper, a first-order stable linear system is used as the pre-specified target dynamical system in order to avoid the problem of finding the solutions of partial differential equations (PDEs) required in the condition (H2) of Theorem 3.1, which is a difficult problem to solve.

$$\dot{\xi}_1 = -k\xi_1 \tag{13}$$

where $\xi_1 \in \mathbb{R}$ denotes the state variable of the target system and k denotes a positive design constant.

3.2.2. *Immersion condition.* This step involves determining the mapping function between the HESM and the selected target dynamical system. In accordance with the selected target systems in (13), a mapping function $\pi : \mathbb{R} \to \mathbb{R} \times \mathbb{R} \times \mathbb{R} \times \mathbb{R}$ is selected as

$$\pi(\xi) := \begin{bmatrix} \pi_1(\xi), & \pi_2(\xi), & \pi_3(\xi), & \pi_4(\xi) \end{bmatrix}^T \tag{14}$$

where $\pi_i(\xi)$, $i = 1, 2, 3, 4$ represents the mapping function that needs to be constructed. Following the condition (H1) of Theorem 3.1, it needs to take account of the following constraints: $\xi_{1e} = x_{1e} = 0$, $\xi_{2e} = i_{de} i_{qe}$, $\xi_{3e} = x_{3e} = i_{qe}$, $\xi_{4e} = i_{qe} i_{fe}$.

From the condition (H2), one of the major problems with the I&I scheme is how to solve the partial differential equation (PDE) (9). The solution to the PDE may be achieved by starting with $x_1 = \pi_1(\xi)$ because the target system (the first-order stable linear system) has the same dynamics as the HESM system. After taking the derivative of x_1, one obtains $\dot{x}_1 = \frac{\partial \pi_1(\xi)}{\partial \xi_1} \dot{\xi}_1$. It is straightforward to choose $\pi_1(\xi) = \xi_1$, from (13); subsequently, we have

$$\dot{x}_1 = \frac{\partial \pi_1(\xi)}{\partial \xi_1} \dot{\xi}_1 \tag{15}$$

where $\frac{\partial \pi_1(\xi)}{\partial \xi_1} = 1$. When focusing on the term $\dot{x}_1 = \dot{\xi}_1 = -k\xi_1$, let us define the mapping functions $\pi_2(\xi) = \pi_2(\xi_1)$, $\pi_3(\xi) = \pi_3(\xi_1)$ and $\pi_4(\xi) = \pi_4(\xi_1)$ which are derived as

$$\dot{x}_1 = \dot{\xi}_1 = -k\xi_1 = -\frac{R_\Omega}{J}(\xi_1 + \omega_r) + \frac{P_n}{J}(L_d - L_q)\pi_2 + \frac{P_n \Phi_a}{J}\pi_3 + \frac{P_n M_f}{J}\pi_4 - \frac{T_l}{J} \tag{16}$$

Following the immersion condition (H2) in (9), $\pi_2(\xi_1)$, $\pi_3(\xi_1)$ and $\pi_4(\xi_1)$ can be determined using the partial differential equation in (16).

From the selection of $\pi(\xi)$, the target dynamics are reduced to the algebraic equations:

$$-k\xi_1 = -\frac{R_\Omega}{J}(\xi_1 + \omega_r) + \frac{P_n}{J}(L_d - L_q)\pi_2(\xi_1) + \frac{P_n \Phi_a}{J}\pi_3(\xi_1) + \frac{P_n M_f}{J}\pi_4(\xi_1) - \frac{T_l}{J} \tag{17}$$

From the expression above, we select a solution of the PDE as follows:

$$\pi_2(\xi_1) = \frac{J}{3P_n(L_d - L_q)}\left(-k\xi_1 + \frac{R_\Omega}{J}(\xi_1 + \omega_r)\right) \tag{18}$$

$$\pi_3(\xi_1) = \frac{J}{3P_n\Phi_a}\left(-k\xi_1 + \frac{R_\Omega}{J}(\xi_1 + \omega_r) + \frac{3T_l}{J}\right) \tag{19}$$

$$\pi_4(\xi_1) = \frac{J}{3P_nM_f}\left(-k\xi_1 + \frac{R_\Omega}{J}(\xi_1 + \omega_r)\right) \tag{20}$$

It is seen that ξ_1 is directly involved with the mapping functions π_3.

3.2.3. *Implicit manifold.* Following the selection of the mapping functions π_2, π_3 and π_4, it immediately follows from the condition (H3) that the manifold $\mathcal{M}$ is implicitly represented by $\mathcal{M} = \{x \in \mathbb{R}\times\mathbb{R}\times\mathbb{R}\times\mathbb{R} |\ \phi(x) = 0\}$ where the mapping $\phi(x) = [\phi_1(x), \phi_2(x), \phi_3(x)]^T$ is defined as

$$\phi_1(x) = x_2x_3 - \pi_2(x_1) = x_2x_3 - \frac{J}{3P_n(L_d - L_q)}\left(-kx_1 + \frac{R_\Omega}{J}(x_1 + \omega_r)\right) \tag{21}$$

$$\phi_2(x) = x_3 - \pi_3(x_1) = x_3 - \frac{J}{3P_n\Phi_a}\left(-kx_1 + \frac{R_\Omega}{J}x_1 + \frac{3T_l}{J}\right) \tag{22}$$

$$\phi_3(x) = x_3x_4 - \pi_4(x_1) = x_3x_4 - \frac{J}{3P_nM_f}\left(-kx_1 + \frac{R_\Omega}{J}(x_1 + \omega_r)\right) \tag{23}$$

3.2.4. *Manifold attractivity and trajectory boundedness.* In this subsection, the controller $u = \varphi(x, z) = [\varphi_d(x, z), \varphi_q(x, z), \varphi_f(x, z)]^T$ is selected to ensure that all the closed-loop system's signals are bounded and eventually approach the manifold $\mathcal{M}$. Let us introduce $z = [z_1, z_2, z_3]^T$ where $z_1 = \phi_1(x) = x_2x_3 - \pi_2(x)$, $z_2 = \phi_2(x_1) = x_3 - \pi_3(x_1)$ and $z_3 = \phi_3(x_1) = x_3x_4 - \pi_4(x_1)$ as the off-the-manifold coordinate; substituting $\dot{x}_1$ into the expressions below, it is straightforward to obtain

$$\begin{aligned}
\dot{z}_1 &= \dot{x}_2x_3 + x_2\dot{x}_3 - \dot{\pi}_2(x_1)\\
&= f_2(x)x_3 + (f_3(x) + g_{32}u_q)x_2 + g_{21}(x)x_3\varphi_d(x, z) + g_{23}(x)x_3\varphi_f(x, z) - \frac{\partial\pi_2}{\partial x_1}\dot{x}_1\\
\dot{z}_2 &= \dot{x}_3 - \dot{\pi}_3(x_1)\\
&= f_3(x) + g_{32}(x)\varphi_q(x, z) - \frac{\partial\pi_3}{\partial x_1}\dot{x}_1\\
\dot{z}_3 &= \dot{x}_4 - \dot{\pi}_4(x_1)\\
&= f_3(x)x_3 + (f_3(x) + g_{32}u_q)x_4 + g_{41}(x)x_3\varphi_d(x, z) + g_{43}(x)x_3\varphi_f(x, z) - \frac{\partial\pi_4}{\partial x_1}\dot{x}_1
\end{aligned}$$

According to the condition (12) that ensures the boundedness of trajectories of the off-the-manifold coordinate $z = [z_1, z_2, z_3]^T$ and $\lim_{t\to+\infty} z_1(t) = \lim_{t\to+\infty} z_2(t) = \lim_{t\to+\infty} z_3(t) = 0$, we take $\dot{z}_1 = -\gamma_1 z_1$, $\dot{z}_2 = -\gamma_2 z_2$ and $\dot{z}_3 = -\gamma_3 z_3$, $\gamma_1 > 0$, $\gamma_2 > 0$, $\gamma_3 > 0$ to ensure the exponential convergence of z toward zero. Thus, one obtains

$$\dot{z}_1 = -\gamma_1 z_1 = f_2(x)x_3 + (f_3(x) + g_{32}u_q)x_2 + g_{21}(x)x_3\varphi_d(x, z) + g_{23}(x)x_3\varphi_f(x, z) - \frac{\partial\pi_2}{\partial x_1}\dot{x}_1$$

$$\dot{z}_2 = -\gamma_2 z_2 = f_3(x) + g_{32}(x)\varphi_q(x, z) - \frac{\partial\pi_3}{\partial x_1}\dot{x}_1$$

$$\dot{z}_3 = -\gamma_3 z_3 = f_3(x)x_3 + (f_3(x) + g_{32}u_q)x_4 + g_{41}(x)x_3\varphi_d(x, z) + g_{43}(x)x_3\varphi_f(x, z) - \frac{\partial\pi_4}{\partial x_1}\dot{x}_1$$

3.2.5. *The control law.* Based on Theorem 3.1 and the expression above, the developed control law is chosen as follows.

$$u = \varphi(x,z) = \left[\ \varphi_d(x,z),\quad \varphi_q(x,z),\quad \varphi_f(x,z)\ \right]^T \tag{24}$$

with $\varphi_d(x,z) = -\frac{1}{\Delta}(L_d v_1 + M_f v_2)$, $\varphi_q(x,z) = \frac{\left(-\gamma_2 z_2 - f_3 + \frac{\partial \pi_3}{\partial x_1}\dot{x}_1\right)}{g_{32}(x)}$, $\varphi_f(x,z) = -\frac{1}{\Delta}(M_f v_1 + L_f v_2)$, where

$$\frac{\partial \pi_2}{\partial x_1} = \frac{J}{3P_n(L_d - L_q)}\left(-k + \frac{R_\Omega}{J}\right), \quad \frac{\partial \pi_3}{\partial x_1} = \frac{J}{3P_n\Phi_a}\left(-k + \frac{R_\Omega}{J}\right),$$
$$\frac{\partial \pi_4}{\partial x_1} = \frac{J}{3P_n M_f}\left(-k + \frac{R_\Omega}{J}\right), \quad v_1 = \frac{-\gamma_1 z_1 - (f_3(x) + g_{32}u_q)x_2 + \frac{\partial \pi_2}{\partial x_1}\dot{x}_1}{x_3} - f_2(x),$$
$$v_2 = \frac{-\gamma_3 z_3 - (f_3(x) + g_{32}u_q)x_4 + \frac{\partial \pi_4}{\partial x_1}\dot{x}_1}{x_3} - f_4(x), \quad \Delta = KM_f^2 - KL_dL_f \neq 0,$$

where $\dot{x}_1$ is given in (3). Notably, once the control input u is employed to drive the closed-loop dynamics toward the manifold, the system behaves like the target dynamics.

To satisfy the condition (H4), it is necessary to prove that all signals of the closed-loop system with the proposed control law $\varphi(x,\phi(x))$, as well as the off-the-manifold coordinate z, are bounded as given below:

$$\begin{aligned}
\dot{x}_1 &= -\frac{R_\Omega}{J}(x_1 + \omega_r) + \frac{P_n}{J}(L_d - L_q)x_2x_3 + \frac{P_n\Phi_a}{J}x_3 + \frac{P_nM_f}{J}x_3x_4 - \frac{T_l}{J} \\
&= -\frac{R_\Omega}{J}(x_1 + \omega_r) + \frac{P_n}{J}(L_d - L_q)(z_1 + \pi_2) + \frac{P_n\Phi_a}{J}(z_2 + \pi_3) + \frac{P_nM_f}{J}(z_3 + \pi_4) - \frac{T_l}{J}, \\
\dot{z}_1 &= -\gamma_1 z_1, \\
\dot{z}_2 &= -\gamma_2 z_2, \\
\dot{z}_3 &= -\gamma_3 z_3
\end{aligned} \tag{25}$$

From the selected target dynamical system and the condition (H4), it is easy to observe that x_1 is bounded, and z_1, z_2 and z_3 are the exponentially decaying functions, e.g., $z_i(t) = z_i(0)e^{-\gamma_i t}$, $i = 1,2,3$. Based on the energy function $\mathcal{W} = \frac{1}{2}x_1^2 + \frac{1}{2}\sum_{i=1}^{3} z_i^2$, and some straightforward calculation with Lemma 2.1 $\left(ab \leq \frac{a^2}{4\epsilon} + \epsilon b^2, \epsilon > 0\right)$ and Assumption 2.1, we obtain

$$\begin{aligned}
\dot{\mathcal{W}} &= x_1\dot{x}_1 + z_1\dot{z}_1 + z_2\dot{z}_2 + z_3\dot{z}_3 \\
&= x_1\Bigg(-\frac{R_\Omega}{J}(x_1 + \omega_r) + \frac{P_n}{J}(L_d - L_q)(z_1 + \pi_2) + \frac{P_n\Phi_a}{J}(z_2 + \pi_3) \\
&\quad + \frac{P_nM_f}{J}(z_3 + \pi_4) - \frac{T_l}{J}\Bigg) - \gamma_1 z_1^2 - \gamma_2 z_2^2 - \gamma_3 z_3^2 \\
&= x_1\left(-\frac{R_\Omega}{J}(x_1 + \omega_r) + \frac{P_n}{J}(L_d - L_q)z_1 + \frac{P_n\Phi_a}{J}z_2 + \frac{P_nM_f}{J}z_3 - \frac{T_l}{J}\right) \\
&\quad - \gamma_1 z_1^2 - \gamma_2 z_2^2 - \gamma_3 z_3^2 \\
&= -kx_1^2 + \frac{P_n}{J}(L_d - L_q)x_1z_1 + \frac{P_n\Phi_a}{J}x_1z_2 + \frac{P_nM_f}{J}x_1z_3 - \gamma_1 z_1^2 - \gamma_2 z_2^2 - \gamma_3 z_3^2
\end{aligned} \tag{26}$$

Using some straightforward calculation with Lemma 2.1 $\left(ab \leq \frac{a^2}{4\epsilon} + \epsilon b^2,\ \epsilon > 0\right)$ and Assumption 2.1, we have

$$\begin{aligned}
\dot{\mathcal{W}} \leq &-\left(k - \frac{1}{4\epsilon_1}\left(\frac{P_n(L_d - L_q)}{J}\right)^2 - \frac{1}{4\epsilon_2}\left(\frac{P_n\Phi_n}{J}\right)^2 - \frac{1}{4\epsilon_3}\left(\frac{P_nM_f}{J}\right)^2\right)x_1^2 \\
&- (\gamma_1 - \epsilon_1)z_1^2 - (\gamma_2 - \epsilon_2)z_2^2 - (\gamma_3 - \epsilon_3)z_3^2
\end{aligned} \tag{27}$$

with ϵ_1, ϵ_2, and ϵ_3 as positive design constants.

According to the inequality above, by selecting $k > \frac{1}{4\epsilon_1}\left(\frac{P_n(L_d-L_q)}{J}\right)^2 + \frac{1}{4\epsilon_2}\left(\frac{P_n\Phi_n}{J}\right)^2 + \frac{1}{4\epsilon_3}\left(\frac{P_nM_f}{J}\right)^2$, $\gamma_1 > \epsilon_1$, $\gamma_2 > \epsilon_2$, $\gamma_3 > \epsilon_3$, it can be concluded that $\dot{\mathcal{W}} \leq 0$. Therefore, it immediately follows that $\mathcal{W}(x_1, z_1, z_2, z_3) \leq \mathcal{W}(x_1(0), z_1(0), z_2(0), z_3(0))$, thereby resulting in boundedness of x_1, z_1, z_2, and z_3 together with $\lim_{t\to+\infty} z_1(t) = \lim_{t\to+\infty} z_2(t) = \lim_{t\to+\infty} z_3(t) = 0$. Also, this implies boundedness of $\pi_2(x_1)$, $\pi_3(x_1)$ and $\pi_4(x_1)$. Finally, x_2, x_3 and x_4 are bounded from the fact that $x_2x_3 = z_1 + \pi_2(x_1)$, $x_3 = z_2 + \pi_3(x_1)$ and $x_3x_4 = z_3 + \pi_4(x_1)$.

The following proposition summarizes the I&I control design for the HESM model.

Proposition 3.1. *Under Assumption 2.1, the overall closed-loop system (25) under the developed control law (24) is asymptotically stable in x_e. Also, all the signals of the closed-loop system are bounded.*

Proof: The proof of Proposition 3.1 is on the basis of the arguments given above.

Remark 3.1. *The immersion and invariance (I&I) approach is utilized for the HESM system because it has several benefits over other methods, especially backstepping, including the following. (i) It breaks down the control design problem into smaller subproblems that can be dealt with more easily in some cases. For example, in order to obtain the actual control law for high-order systems, the backstepping design requires the repeated derivative of virtual control functions. When the I&I design can determine an appropriate target system that captures the required system behavior, the design approach is simplified, even when developed for the same high-order systems. (ii) Not necessary is knowledge of a (control) Lyapunov function. Evidently, the backstepping approach must develop a virtual control function to stabilize the subsystem using the Lyapunov function at each design step. For the presented I&I design, the Lyapunov function will be used to demonstrate that all closed-loop system signals are bounded.*

The proposed approach employed in this paper can also effectively address the following drawbacks of the current nonlinear control systems: (i) it does not necessitate the repeating derivative of virtual control functions and knowledge of a (control) Lyapunov function, as opposed to backstepping; (ii) it is systematically designed, whereas slide mode design focuses on finding an appropriate sliding surface; (iii) it can be immediately constructed with the use of nonlinear control theory, regardless of the linearization techniques applied close to the operational point; and (iv) the feedback linearization approach requires finding the output function that transforms the original system to normal form, resulting in a time-consuming and laborious computation, whereas the I&I method does not.

4. **Simulation Results.** This section presents performance verification and indicates the effectiveness of the developed controller. The proposed controller is evaluated via the simulations. Also, the performance of the proposed control scheme is evaluated in MATLAB environment.

The physical parameters (pu.), the controller parameters, and initial parameters used for this HESM model are as follows.

- The parameters of the HESM model [5] in (1) are $R = 2.875\ \Omega$, $R_f = 2.5\ \Omega$, $L_d = 0.0085$ H, $L_q = 0.008$ H, $L_f = 0.008$ H, $M_f = 0.0025$ H, $R_\Omega = 0.0002$ Nms, $P_n = 2$, $\Phi_a = 0.175$ Wb, $J = 0.0008$ kgm^2, $\omega_r = 500$ rad/s.
- The control parameters of the proposed controller are $k = \gamma_2 = \gamma_3 = \gamma_4 = 20$, $\epsilon_1 = \epsilon_2 = \epsilon_3 = 1$.
- Initial parameters $\omega_0 = 1$ rad/s, $i_{d0} = i_{q0} = i_{f0} = 1$ A.

The time domain simulations are carried out via MATLAB environment. To evaluate the effectiveness and feasibility of the designed controller, as given in (24), the performance of the proposed controller is compared with that of the backstepping controller [10], as given in (28).

- Backstepping controller (BSC) [10]

$$\begin{cases} u_q(x) &= \dfrac{1}{g_{32}(x)}\left(-c_3 y_3 - f_3(x) + \dot{\alpha}_3 - \dfrac{P_n \Phi_a z_1}{J}\right) \\ u_d(x) &= -\dfrac{1}{\Delta}(L_d \bar{v}_1 + M_f \bar{v}_2) \\ u_f(x) &= -\dfrac{1}{\Delta}(M_f \bar{v}_1 + L_f \bar{v}_2) \end{cases} \tag{28}$$

where $y_1 = x_1 - \omega_r$, $y_2 = x_2 - \alpha_2$, $y_3 = x_3 - \alpha_3$, $y_4 = x_4 - \alpha_4$, $\alpha_2 = \alpha_4 = 0$, $\alpha_3 = \frac{J}{P_n \Phi_a}\left(-c_1 y_1 + \frac{R_\Omega}{J}(z_1 + \omega_r) + \frac{T_L}{J}\right)$, $\bar{v}_1 = -c_2 y_2 - \frac{P_n}{J}(L_d - L_q) i_q y_1 - f_2(x)$, $\bar{v}_2 = -c_4 y_4 - \frac{M_f P_n}{J} i_q y_1 - f_4(x)$, $\Delta = K M_f^2 - K L_d L_f \neq 0$. The controller parameters of the backstepping control law are chosen as follows: $c_i = 20$, $i = 1, 2, 3, 4$.

Further, the load torque used in the simulations is as follows:

$$T_l = \begin{cases} 0.1, & 0 \leq t \leq 0.6 \text{ s} \\ 1.5, & 0.6 \text{ s} < t \leq 1 \text{ s} \\ 0.1, & 1 \text{ s} < t \leq 1.5 \text{ s} \end{cases}$$

The followings are the simulation results, which are presented and discussed. Figure 1 shows time responses of the HESM rotor speed ω, the d-axis current i_d, the q-axis current i_q, and the additional excitation current i_f under the proposed controller and backstepping controller. Figure 2 illustrates time histories of the HESM rotor speed tracking error $x_1 - \omega_r$, the d-axis current tracking error z_1, the q-axis current tracking error z_2, and

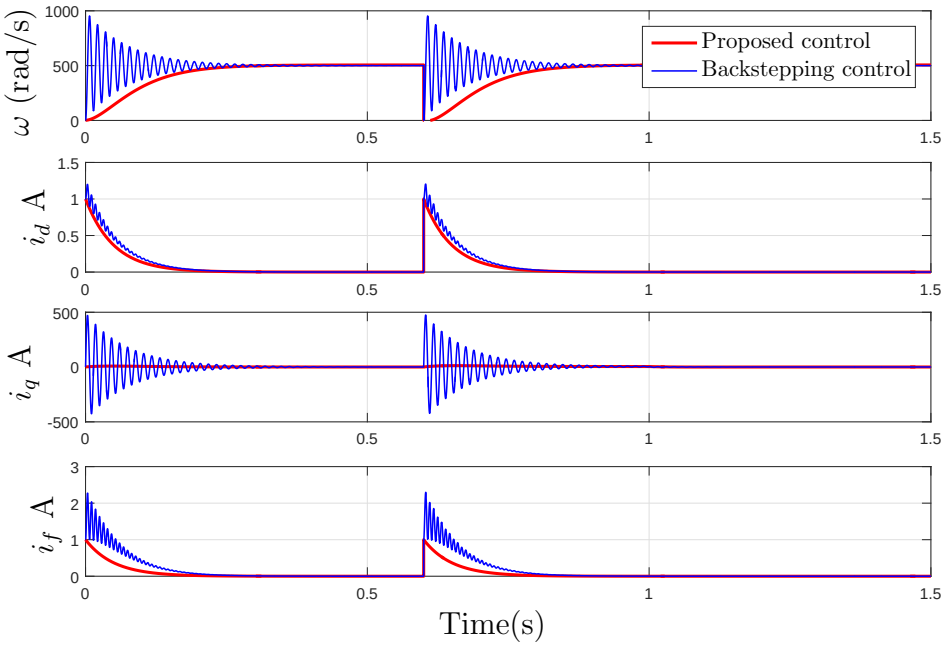

FIGURE 1. Controller performance – Rotor speed ω, d-axis current i_d, q-axis current i_q and additional excitation current i_f under the proposed controller and backstepping controller

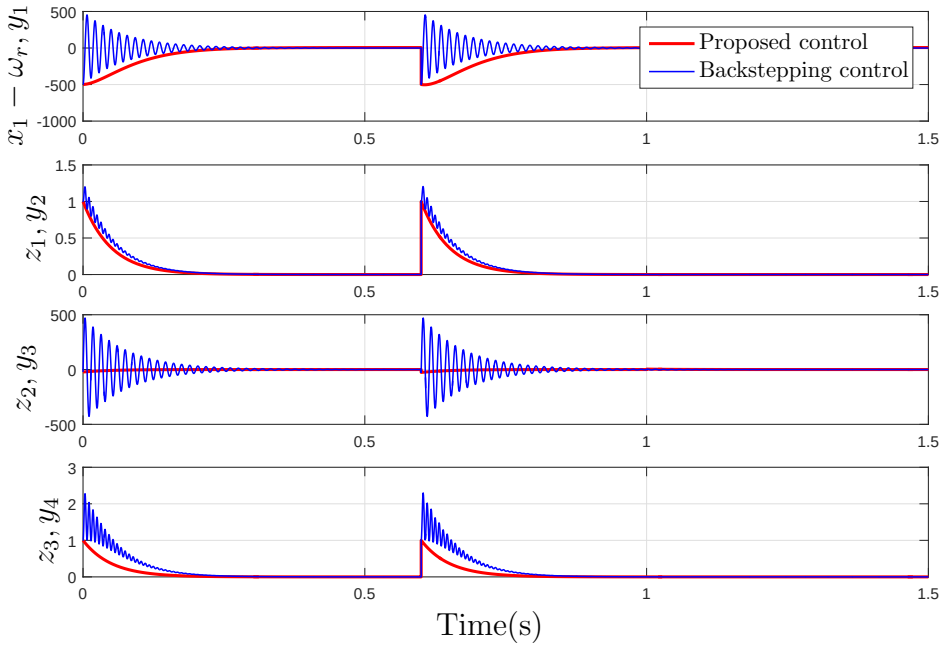

FIGURE 2. Controller performance – Time responses of rotor speed tracking error $x_1 - \omega_r$, d-axis current tracking error z_1, q-axis current tracking error z_2 and additional excitation current tracking error z_3 under the proposed controller and backstepping controller

the additional excitation current tracking error z_3 under the proposed controller and backstepping controller.

From these figures, it is clear that the provided control law improves dynamic performance more than the backstepping method. It can be observed from Figure 2 that all tracking errors $x_1 - \omega_r$, z_1, z_2, and z_3 of the proposed control can fast converge to zero compared with those of the backstepping. For these time responses, it is obvious that dynamic (transient) performances, such as fast reduction of oscillatory overshoot and shorter settling time, are enhanced. It is noted that, even if the backstepping controller can meet the conditions outlined in the paper's goal, it provides poorer transient performance when compared to the proposed controller. Also, according to Equations (21)-(23), the off-the-manifold coordinates z_1, z_2 and z_3 depict the manifold $\mathcal{M}$ implicitly described by $\phi(x) \to 0$, as expected.

In summary, the simulation results show that the provided method performs better than the backstepping design and provides satisfactory dynamic performance as evidenced by the quick dampening of oscillations across all time trajectories. It is evident that the HESM rotor speed can track the reference rotor speed ω_r. Further, with the suggested control strategy, all the signals of the closed-loop dynamics are bounded.

5. **Conclusion.** In this study, the nonlinear controller has been designed using the immersion and invariance control technique. The simulation results have suggested that the proposed control mechanism is effective. It can not only keep all signals of closed-loop system trajectories stable and bounded, but also make the rotor speed tracking error rapidly converge to zero according to the desired requirements. In terms of improved dynamic control performance, the presented approach surpasses the backstepping method. Furthermore, the findings demonstrate that the proposed controller is effective at dealing with the rotor speed tracking problem and enhancing transient performance in the face of

abrupt load torque changes. Future research will focus on how to implement this strategy to develop an adaptive immersion and invariance control method for the HESM model with unknown parameters. The implementation of this approach to design a finite-time command filtered backstepping controller [22] for the HESM model will also be the subject of future research.

REFERENCES

[1] Y. P. Dou, *Design Research of Hybrid Excitation Synchronous Generator*, Ph.D. Thesis, Nanjing University of Aeronautics and Astronautics, Nanjing, China, 2002.

[2] C. Zhao and Y. Yan, A review of development of hybrid excitation synchronous machine, *Proc. of the IEEE International Symposium on Industrial Electronics*, Dubrovnik, Croatia, pp.857-862, 2005.

[3] S. Hlioui, Y. Amara, E. Hoang, M. Lecrivain and M. Gabsi, Overview of hybrid excited synchronous machines technology, *Proc. of 2013 International Conference on Electrical Engineering and Software Applications*, Hammamet, Tunisia, pp.1-10, 2013.

[4] S. Hlioui, M. Gabsi, H. Ben Ahmed, G. Barakat, Y. Amara, F. Chabour and J. J. H. Paulides, Hybrid excited synchronous machines, *IEEE Transactions on Magnetics*, vol.58, no.2, 2022.

[5] Q. Xie, Z. Han and H. Kang, Adaptive backstepping control for hybrid excitation synchronous machine with uncertain parameters, *Expert Systems with Applications*, vol.37, pp.7280-7284, 2010.

[6] G. Rigatos, P. Siano, P. Wira, M. Abbaszadeh and V. Ambrozic, Nonlinear $\mathcal{H}_\infty$ control for hybrid excited synchronous generators, *Proc. of 2020 IEEE 14th International Conference on Compatibility, Power Electronics and Power Engineering (CPE-POWERENG)*, Setubal, Portugal, 2020.

[7] X. Sun, L. Meng, J. Liang and S. Li, Hybrid excitation synchronous motor feedback linearization decoupling sliding mode control, *Proc. of 2019 22nd International Conference on Electrical Machines and Systems (ICEMS)*, Harbin, China, 2019.

[8] A. Astolfi and R. Ortea, Immersion and invariance: A new tool for stabilization and adaptive control of nonlinear systems, *IEEE Transactions on Automatic Control*, vol.48, no.4, pp.590-606, 2003.

[9] A. Astolfi, D. Karagiannis and R. Oreta, *Nonlinear and Adaptive Control Design with Applications*, Springer-Verlag, London, 2007.

[10] M. Krstic, I. Kanellakopoulos and P. Kokotivic, *Nonlinear and Adaptive Control Design*, John Wiley & Sons, New York, 1995.

[11] A. Kanchanahanathai, V. Chankong and K. A. Loparo, Nonlinear generator excitation and superconducting magnetic energy storage control for transient stability enhancement via immersion and invariance, *Transactions of Institute of Measurement Control*, vol.37, no.10, pp.1217-1231, 2015.

[12] A. Kanchanaharuthai, Nonlinear adaptive immersion and invariance control for power systems with SMES, *International Journal of Innovative Computing, Information and Control*, vol.12, no.4, pp.1129-1140, 2016.

[13] A. Kanchanahanathai, Immersion and invariance-based nonlinear dual-excitation and steam-valving control of synchronous generators, *International Transactions on Electrical Energy Systems*, vol.24, no.12, pp.1671-1687, 2014.

[14] A. Kanchanaharuthai, Immersion and invariance-based nonlinear coordinated controller for generator excitation and static synchronous compensator of power systems, *Electric Power Component and Systems*, vol.42, no.10, pp.1004-1015, 2014.

[15] A. Kanchanaharuthai, Immersion and invariance-based coordinated generator excitation and SVC control for power systems, *Mathematical Problem of Engineering*, Article ID 720570, 2014.

[16] M. H. Sabzalian, A. Mohammadzadeh, S. Lin and W. Zhang, New approach to control the induction motors based on immersion and invaraince technique, *IET Control Theory and Applications*, vol.13, no.10, pp.1466-1472, 2019.

[17] Q. Han and X. Liu, Robust I&I adaptive control for a class of quadrotors with disturbances, *IEEE Access*, vol.8, pp.216519-216528, 2020.

[18] M. Tavan, K. Sabahi, A. Hajizadeh, M. N. Soltani and K. Jessen, Overcoming the detectability obstacle in adaptive output feedback control of DC-DC boost converter with unknown load, *IEEE Transactions on Control Systems Technolongy*, vol.29, no.6, pp.2678-2686, 2021.

[19] W. Hao, B. Xian and T. Xie, Fault tolerant position tracking control design for a tilt tri-rotor unmanned aerial vehicle, *IEEE Transactions on Industrial Electronics*, vol.69, no.1, pp.604-612, 2020.

[20] L. Gong, M. Wang and C. Zhu, Immersion and invariance manifold adaptive control of the DC-link voltage in flywheel energy storage system discharge, *IEEE Access*, vol.8, pp.144489-144502, 2020.

[21] S. Poonyanirun and A. Kanchanahanathai, Congestion tracking control for wireless TCP/AQM network via immersion and invariance, *Asian J. Control*, pp.1-17, https://doi.org/10.1002/asjc.2824, 2022.

[22] A. Kanchanaharuthai and E. Mujjalinvimut, Finite-time command filtered backstepping control design for power systems with superconducting magnetic energy storage system, *International Journal of Innovative Computing, Information and Control*, vol.17, no.3, pp.873-885, 2021.

Author Biography

Ekkachai Mujjalinvimut received the B.Eng., M.Eng. and D.Eng. degrees in the Department of Electrical Engineering from King Mongkut's University of Technology Thonburi (KMUTT), Bangkok, Thailand, in 2007, 2009 and 2016, respectively. He is currently an Assistant Professor at the Department of Electrical Engineering, KMUTT, Thailand. His current research interests include switched mode power supplies, and digital control of power electronic converters together with power system stability and control.

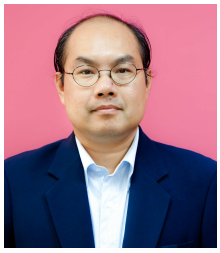

Adirak Kanchanaharuthai received the B.Eng. degree in Control Engineering from King Mongkut's Institute of Technology Ladkrabang, Thailand, the M.Eng. degree in Electrical Engineering from Chulalongkorn University, Thailand, and the Ph.D. degree in Systems and Control Engineering from Case Western Reserve University, Cleveland, OH, USA, in 1995, 1997, and 2012, respectively. Currently, he is an Associate Professor at the Department of Electrical Engineering, Rangsit University, Thailand. His main research interests include power system dynamics, stability and control, renewable energy systems, energy storage systems, and applications of nonlinear control theory to power systems, flexible alternating current transmission systems (FACTS) devices, and congestion tracking control for TCP/AQM network systems.